Polysaccharide Extracted From the Fibrous Residue of the Pseudofruit of Anacardium Occidentale as a Promising Biomaterial for Scaffold Development

Maria Crisnanda Almeida Marques
mariacrisnanda@ufpi.edu.br
Universidade Federal do Piauí
Livio Cesar Cunha Nunes
Universidade Federal do Piauí
Ezequiel da Silva Ferreira
Universidade Federal do Piauí
Edmilson Araújo de Oliveira Junior
Universidade Federal do Piauí
Solange Sousa Santos
Universidade Federal do Piauí
Francisco Mayron de Sousa e Silva
Universidade Federal do Piauí
Matheus Pereira Macêdo
Universidade Federal do Piauí
Thátila Wanessa Vieira de Sousa
Universidade Federal do Piauí
José Lamartine Soares Sobrinho
Federal University of Pernambuco
Francisca Maria Macêdo Pereira
Universidade Federal do Piauí
Jurandy do Nascimento Silva
Universidade Federal do Piauí

Research Article

Keywords: Biopolymers, Anacardium occidentale, Agro-industrial residue, Natural polysaccharide, Scaffold

Posted Date: July 27th, 2026

DOI: https://doi.org/10.21203/rs.3.rs-10436345/v1

Additional Declarations: No competing interests reported.

POLYSACCHARIDE EXTRACTED FROM THE FIBROUS RESIDUE OF THE PSEUDOFRUIT OF *ANACARDIUM OCCIDENTALE* AS A PROMISING BIOMATERIAL FOR SCAFFOLD DEVELOPMENT

Maria Crisnanda Almeida Marques[a]
mariacrisnanda@ufpi.edu.br
Livio Cesar Cunha Nunes[b]
liviocesar@hotmail.com
Ezequiel da Silva Ferreira[c]
es48506@gmail.com
Edmilson Araújo de Oliveira Júnior[d]
eajunior2014@gmail.com
Solange Sousa Santos[a]
solange.santos@ifma.edu.br
Francisco Mayron de Sousa e Silva[a]
mayrondcf@gmail.com
Matheus Pereira Macêdo[b]
matheus.macedo@ufpi.edu.br
Thátila Wanessa V. de Sousa[d]
thatila.vieira@ufpi.edu.br
José Lamartine Soares Sobrinho[e]
jose.ssobrinho@ufpe.br
Francisca Maria Macêdo Pereira[f]
francisca.macedo@ufpi.edu.br
Jurandy do Nascimento Silva[f]
jurandy@ufpi.edu.br
[a]Postgraduate Program in Pharmaceutical Sciences, Federal University of Piauí, 64049-550, Teresina, Piauí, Brazil.
[b]Department of Pharmacy, Federal University of Piauí, 64049-550, Teresina, Piaui, Brazil.
[c]Postgraduate Program In Materials Science And Engineering, Federal University of Piauí, 64049-550, Teresina, Piauí, Brazil.
[d]Interdisciplinary laboratory of advanced materials, Federal University of Piauí, 64049-550, Teresina, Piauí, Brazil.
[e]Department of pharmaceutical sciences, Federal University of Pernambuco, 50740520, Recife, Pernambuco, Brazil.
[f]Chemistry department, Federal University of Piauí, 64049-550, Teresina, Piauí, Brazil.
*Corresponding author: Tel (86) 998495619
https://orcid.org/0000-0002-0554-001X

ABSTRACT

Scaffolds are three-dimensional porous matrices used as supports for biomedical applications; they must be biocompatible, biodegradable, and possess mechanical properties suitable for the site of application. *Anacardium occidentale*, a species native to Brazil, generates a significant volume of waste during the processing of its pseudofruit, which is generally discarded despite its high polysaccharide content. The objective of this study was to extract and characterize the polysaccharide obtained from the fibrous waste of the *A. occidentale* pseudofruit, as well as to use it in the production of scaffolds. The polysaccharide was obtained using the hot-water extraction method followed by ethanol precipitation. Physicochemical characterization included FTIR, SEM, XRF, and TGA. Biological characterization included in vitro antioxidant and antimicrobial activity assays and toxicity tests. To produce the scaffold, hydrogels were prepared using a polymer blend containing *A. occidentale* polysaccharide. After 24 h of drying, the hydrogels were freeze-dried. The morphology of the scaffolds was evaluated by computed microtomography and SEM, while ex vivo mucoadhesion was determined using porcine vaginal tissue. The extraction yield was 2.54 ± 1.54%. The polysaccharide exhibited characteristic bands of typical functional groups, a lamellar morphological structure, a predominance of K, Ca, and P, and good thermal stability. Antioxidant activity showed a EC_{50} of 0.5688 ± 0.01 mg/mL, while the assays indicated low toxicity. The scaffolds exhibited porosity greater than 80%, with a network of interconnected pores and moderate mucoadhesiveness. The results demonstrate that the polysaccharide from *A. occidentale* is a promising biomaterial for the development of scaffolds derived from agroindustrial waste.

Keywords: Biopolymers, *Anacardium occidentale*, Agro-industrial residue, Natural polysaccharide, Scaffold.

1. Introduction

A polymeric scaffold is a three-dimensional matrix that serves as a support for cells, promoting tissue regeneration [1], and also allows for the incorporation and release of therapeutic substances such as drugs, growth factors, and bioactive molecules, making it highly relevant for tissue engineering and more targeted treatments [2,3].

They can be produced from synthetic or natural polymers; in recent years, the search for sustainable materials has made natural polymers a more viable option, and they also exhibit greater biocompatibility and bioactivity than synthetic polymers [4]. For scaffold production, natural polymers can include peptides, proteins,

and polysaccharides; the latter can be obtained from animal and plant sources, making them suitable for scaffold production without the need for chemical modifications [5].

The variety of sources and the abundance of polysaccharides are other characteristics that favor their use; recent trends have encouraged the production of this polymer through the reuse of agro-industrial waste [6]. They are increasingly being used in the production of scaffolds due to their porosity, water retention capacity, biocompatibility with the extracellular matrix, biodegradability, low immunogenicity, and low cost [7,8].

The species *Anacardium occidentale* produces the cashew nut, which is considered a true fruit, and the pseudofruit—also known as cashew pulp—which is used to make beverages and other products [9]. The processing of the pseudofruit generates a large volume of fibrous waste, which is either discarded or used as animal feed [9], although it is rich in polysaccharides [10] and has potential for extraction and biomedical applications [11].

The pseudofruit pulp consists of cellulose (14.2%), ash (1.07%), reducing sugars (7.25%), starch (4.28%), and moisture (58%) [10]; the pseudofruit exhibits high antioxidant and anti-inflammatory activity; it also has a rich composition of beta-carotene and anthocyanins, indicating that these bioactive compounds may also be present in the bagasse [9,12].

This residue has been used in the production of functional foods [13], xylitol [14], and bioethanol [15]; however, it remains largely unexplored for the extraction of polysaccharides.

Scaffolds can serve as carriers for cells, active substances, and drugs, for combination therapy with tissue regeneration or for targeted drug delivery [16]. Controlled drug release maintains optimal therapeutic levels during treatment, avoiding multiple administrations and increasing the safety and efficacy of treatment [3]. Drug delivery using scaffolds allows for local applications, avoiding systemic distribution and requiring lower doses, thereby minimizing side effects [17].

The incorporation of drugs into scaffolds can occur during production or afterward; mixture loading is the most accessible and easiest technique to perform, consisting of mixing the drug with the polymers followed by the addition of a common solvent [3]. In light of the above, the present study aims to extract and characterize the polysaccharide from the fibrous residue of the *A. occidentale* pseudofruit, as well as to produce and characterize a scaffold from this biomaterial.

2. Materials and Methods

2.1 Plant Material and Reagents

The fibrous residue from the pseudofruit of *Anacardium occidentale* was kindly provided by Fitofit (Teresina, PI) (SISGEN: ABD61DA). The main reagents used include: 94% PA ethanol (Dinâmica), 2,2-diphenyl-1-picrylhydrazyl (DPPH•) free radical (Sigma-Aldrich), ascorbic acid (Vetec), Trolox® (Sigma-Aldrich), xanthan gum (Dinâmica), fluconazole (Aché), Ocean Tech® synthetic sea salt, vitamins B1 and B12 (Sigma-Aldrich), culture medium (Sigma-Aldrich), absolute alcohol (Dinâmica), and methanol (Dinâmica). The other chemicals used in this study were of analytical grade.

2.2 Polysaccharide Extraction

To investigate the optimal extraction conditions, a 2^3 factorial design was conducted to test the variables: time, temperature, and concentration of the fibrous residue, as shown in Table 1. The experiment selected as the standard was the one that yielded the highest yield, using 5% (w/v) of the plant material dissolved in distilled water and heated to 90 °C.

It was then agitated at 800 rpm for 10 h. After this step, the material was filtered, and the resulting liquid was precipitated with 94% PA ethyl alcohol in a 1:4 ratio (ethanol extract). The precipitated liquid was then centrifuged, and the collected supernatant was dried in an oven at 40 °C for approximately 24 h [64]; subsequently, the particle size was standardized using a sieve and pestle, and the polysaccharide was stored in a lidded container and kept at room temperature. It was stored in a sealed container and kept at room temperature.

The yield was calculated using the following equation:

$$R = (P_s / P_r) \times 100 \ (1)$$

Onde: PS= Dry polysaccharide weight; PR = Weight of the fibrous residue used in polysaccharide extraction.

2.3 Physical and Chemical Characterization

2.3.1 Organoleptic Analysis (Appearance, Color, and Odor)

The initial physical characterization of the polysaccharide was performed by organoleptic analysis, as described in the Brazilian Pharmacopoeia [9]. The dried sample was observed under diffused natural light on a white surface and evaluated for color, odor, and visual morphology. Color was described based on a standardized visual scale; physical form was evaluated for homogeneity and the presence of visible aggregates or fibers; and odor was assessed by direct inspection.

2.3.2 Moisture Determination

Moisture content was determined using a Marte® moisture analyzer, model ID200. The samples were weighed individually and dried at a temperature of 105 °C, in triplicate, for 30 minutes each. For each analysis, a 1-g sample of the polysaccharide was used. Moisture content was calculated as the difference between the initial and final masses of the samples. The following formula was used to determine the moisture content (M%) present in the sample:

$$M\% = (P_1 - P_2) / P_1 \times 100 \quad (2)$$

Onde: M% = Moisture content; P1 = Initial mass; P2 = Final dough.

2.3.3 pH Determination

The pH was determined as described in the Brazilian Pharmacopoeia, 7th edition [9], using a pH meter properly calibrated with standard buffer solutions (pH 4.0 and 7.0). A 1% (w/v) aqueous solution of the polysaccharide was prepared and stirred magnetically for 30 minutes at room temperature.

2.3.4 Determination of Solubility

Solubility was assessed according to the criteria established by the Brazilian Pharmacopoeia, 7th edition [9], using water, ethanol, and methanol as solvents. In each test, 1 g of polysaccharide was subjected to the gradual addition of the solvent under agitation until complete dissolution. The required volume was recorded, and the substance was classified as “soluble,” “slightly soluble,” or another corresponding term, in accordance with the descriptive terms for solubility presented in the pharmacopoeia.

2.3.5 Determination of the intumescence index

The method described in the Brazilian Pharmacopoeia [9] was used. One gram of the dry sample was weighed and transferred to a 25-ml measuring cylinder, in triplicate. Next, 25 mL of water was added, and the

sample was shaken every 10 minutes for one hour. The mixture was allowed to stand for three hours at room temperature. The volume, in milliliters, occupied by the plant material was measured and subtracted from the initial volume.

$$Swelling = (V_f - V_0) / m \quad (3)$$

Onde: Vf = final volume occupied by the material after hydration (in mL); Vo = initial volume of water added (in mL); m = dry sample mass (in g).

2.3.6 Characterization of the polysaccharide

The polysaccharide was characterized using Fourier-transform infrared spectroscopy (FTIR), scanning electron microscopy (SEM), X-ray fluorescence (XRF), and thermogravimetric analysis (TG).

2.3.7 Infrared spectroscopy

FTIR analysis was performed using a PerkinElmer Spectrum 100 spectrometer, operating in the range of 4000 to 400 cm^{-1}, with a resolution of 1 cm^{-1} and 16 accumulated scans per spectrum. The samples were prepared as pellets using dry KBr (1:100 mg) and compressed under hydraulic pressure of approximately 10 metric tons.

2.3.8 Scanning electron microscopy

The morphology of the polysaccharide was analyzed by SEM using an FEI Quanta FEG 250 instrument equipped with a field emission gun (FEG). The samples, which had been dried beforehand, were mounted on aluminum stubs using carbon adhesive tape. The micrographs were obtained at different magnifications, under an acceleration voltage ranging from 1 to 30 kV and a chamber pressure below 10^{-4} Pa. The images were processed using ImageJ® (National Institutes of Health, Bethesda, MD, USA) to optimize enhancement and contrast.

2.3.9 Fluorescência de raios X

The elemental composition of the polysaccharide was determined by EDXRF using an Epsilon3-XL (Malvern PANalytical) instrument coupled with Omnian analytical software. The system used an X-ray tube with a rhodium (Rh) anode, operating at 50 kV and 300 μA, with a scan time of 10 minutes per sample in ambient air.

2.3.10 Thermogravimetric Analysis (TGA)

TG analysis was performed using a DTG-60 instrument (Shimadzu). Approximately 3.3 mg of the sample was placed in a platinum crucible and heated from 24 to 600°C under an inert nitrogen atmosphere with a flow rate of 100 mL·min^{-1}. The data were processed to obtain the mass loss (TG) and mass loss derivative (DTG) curves.

2.3.11 Biological activity

The biological characterization of the polysaccharide was performed using tests for antioxidant and antimicrobial activity and toxicity in an Artemia salina model.

2.3.12 Antioxidant activity

To perform the analyses, 1.5 mL of the DPPH• radical ethanol solution (6×10^{-5} M) and a 0.5 mL aliquot of the samples containing serial concentrations were added. Measurements were taken using a UV-Vis spectrophotometer (517 nm) 30 minutes after the start of the reaction. The determinations were performed in triplicate (n = 3), along with a negative control (without antioxidant) and two positive controls (standards: ascorbic acid and Trolox®, natural and synthetic, respectively). The decrease in the optical density reading of the samples was correlated with the control, and the percentage of sample decolorization (inhibition of the DPPH• radical) was calculated using the following formula [8,79]:

$$Inhibition\ (\%) = (A\_c - A\_a) / A\_c \times 100\ (4)$$

Where, Abscont = control absorbance, Absamos = sample absorbance. In addition to the percentage of inhibition, the concentration required to inhibit 50% of the radical was also calculated DPPH• (EC50).

2.3.13 Antibacterial activity

The antimicrobial activities of the *A. occidentale* polysaccharide produced were evaluated against the Gram-negative bacterium Escherichia coli (ATCC 10231) using the broth dilution method. Different concentrations of the *A. occidentale* polysaccharide (100, 50, 25, 10, and 5 µg/mL) were added to the microbial culture at 1×10^6 CFU/mL and incubated at 37 °C for up to 48 h. The above experiment was performed in triplicate [65].

2.3.14 In vivo toxicity

A cytotoxicity test was conducted using Artemia salina Leach. An artificial seawater solution was used as the medium for hatching the dehydrated dormant cysts. The Artemia salina cysts were hatched, and after 48 hours, the nauplii were collected for the bioassays. The polysaccharide was diluted to serial concentrations of 250, 500, 1000, and 2000 µg/mL and tested in quintuplicate, with 10 nauplii added to each tube. After 24 and 48 hours of exposure, the number of surviving nauplii was counted.

They were observed near a light source, and all nauplii exhibiting any type of movement when the tube was gently shaken were considered alive. The results were expressed as LC50, calculated using the statistical method of nonlinear regression, followed by the Standard Error of the Mean and a 95% confidence interval (GraphPad Prism 6.0®) [42,43].

2.3.15 Scaffold production

The scaffolds were produced using a methodology adapted from [1,63]. First, an aqueous solution containing 1% (w/v) *A. occidentale* polysaccharide was prepared, to which different proportions of a second polymer were added, resulting in a polymer blend at concentrations of 0.5%, 1%, and 2% (w/v) (Table 2). The mixture was subjected to mechanical homogenization under constant agitation for approximately 10 minutes, ensuring complete dispersion of the components.

At the end of the mixing process, a hydrogel was obtained and carefully transferred to 96-well plates, with a fixed volume of 400 µL dispensed into each well. The material was kept at room temperature for 24 hours to allow for complete gelation. It was then frozen in liquid nitrogen, followed by lyophilization (model L101, Liotop brand). Additionally, a control scaffold without *A. occidentale* polysaccharide was produced.

Tabela 2 - Experimental design of the scaffold production process.

Code	Composition	Polysaccharide from the fibrous residue of *A. occidentale* (%)	Xanthan gum (%)	Antifungal
SCF-C1	Control	X	0,5%	X
SCF-C2	Control	X	1%	X
SCF-C3	Control	X	2%	X
SCF-P1	Test	1%	0,5	X
SCF-P2	Test	1%	1%	X
SCF-P3	Test	1%	2%	X

Legenda: SCF-C: Control scaffold; **SCF-P**: Scaffold containing *A. occidentale* polysaccharide.

2.3. Physical Characteristics

The physical characteristics of the scaffolds were analyzed through visual inspection and measurements. The parameters analyzed included size, shape, color, and odor. The dimensions of the scaffold were measured at three distinct points on each unit using a caliper; diameter and thickness were expressed in millimeters, and the results were presented as mean ± standard deviation, calculated from three units.

2.3.17 Computed Microtomography

The three-dimensional characterization of the internal structure of the scaffolds was performed using micro-computed tomography (micro-CT) with a SkyScan 1272 scanner (Bruker, Belgium). The samples were analyzed without a filter, at a voltage of 50 kV and a current of 200 µA, with a pixel resolution of 5.7 µm. Six scaffold samples were analyzed, divided into three groups (SCFP1, SCFP2, and SCFP3), with two replicates per group. The acquired images had dimensions of 500 × 500 pixels (width × height), and a total of 200 slices contained within the Volume of Interest (VOI) were considered for the quantification of structural parameters. Image reconstruction and porosity analysis were performed using CTAn software (Bruker), and the average porosity of each sample was calculated.

2.3.18 Scanning electron microscopy

The scaffolds were analyzed by SEM using a Tescan VEGA 3 instrument. The samples were mounted on the surface of an aluminum holder using double-sided carbon tape and metallized with a thin layer of gold. The micrographs were obtained at different magnifications, under an acceleration voltage of 10 kV, high-vacuum (HiVac) chamber pressure, and a working distance ranging from 8.69 to 8.83 mm. The images were processed using ImageJ® (National Institutes of Health, Bethesda, MD, USA) to optimize brightness and contrast.

2.3.19 Ex vivo mucoadhesion study

For this study, porcine vaginal mucosa was used as a model; all procedures were guided by the ethical principles established by the National Council for the Control of Animal Experimentation (CONCEA), in accordance with current national legislation (Resolution No. 55, dated October 5, 2022). The vagina was obtained from a local slaughterhouse and removed from a slaughtered animal. After extraction, the tissue was transported on ice and washed with phosphate-buffered saline adjusted to a pH of 4.5 [n].

The experiment was conducted in triplicate using a TA-XT plus texture analyzer (TA Instruments®, United Kingdom), equipped with a 5-kg load. The samples were secured to an analytical probe (p/10), with an area of 0.785 cm², using double-sided tape. The vaginal tissue was secured to the lower platform of the instrument and, prior to each test, was moistened with 50 µL of simulated vaginal fluid heated to 37 °C.

The tests were performed at a speed of 0.5 mm/s for the pre-test and test phases, and 5 mm/s for the post-test phase, applying a force of 0.2 N to the vaginal mucosa for 30 seconds. The force required to separate the tape containing the sample from the tissue surface over the area covered by the sample was measured (Equation 5), which represents the displacement force or mucoadhesive force (N/cm²).

$$P = F_0 / A_0 \quad (4)$$

Where: F0 = force required to detach the sample from the mucosal surface; A0 = area covered by the polymer.

3. RESULTS AND DISCUSSION

3.1 Polysaccharide extraction

The yield of the polysaccharide obtained was 2.54 ± 1.54%, which is lower than that reported by Sabino et al. (2020), who achieved 7% using hot-water extraction under similar conditions of time, temperature, and solvent. However, the protocol described by these authors includes additional steps, such as the removal of the lipid fraction and a second, prolonged extraction of the water-soluble fraction (16 h at 50 °C), which significantly contributes to the increase in yield. Hot-water extraction followed by ethanol precipitation is the most widely used method for obtaining polysaccharides, as it is relatively simple and does not require sophisticated equipment. Although a large volume of ethanol is required, it can be recovered by distillation, thereby reducing the impact of solvent consumption [36].

Among the main limitations of this method are the low yield—since water preferentially solubilizes surface polysaccharides—and the longer time required for the extraction process [81]. Nevertheless, adopting this approach was strategic, as it simulates a step already performed by the partner company responsible for supplying the waste, which was originally used only for washing the waste.

The sample had a homogeneous granular appearance, a yellowish color, and was odorless. The moisture content was determined to be 6.57 ± 0.05%, a value considered low and favorable for the stability of polysaccharides, as it contributes to their preservation [31]. The pH of the aqueous polysaccharide solution was 6.94 ± 0.34, indicating a slightly acidic to nearly neutral character.

This parameter is relevant because it has a direct influence on physicochemical properties, such as polymer viscosity [53]. According to the Brazilian Pharmacopoeia [9], the polysaccharide was soluble in water and had low solubility in organic solvents, such as ethanol and methanol. This behavior is consistent with the extraction method used, which is based on the aqueous solubility of polysaccharides. The high affinity for water can be attributed to the abundance of hydroxyl groups in the structure, which promote hydrophilic interactions [25,46].

The swelling index, which reflects the polysaccharide's ability to absorb water and increase in volume, was 5 mL/g. This value indicates that the material is capable of absorbing approximately five times its dry weight in water, indicating moderate water-retention capacity. This property is also enhanced by the presence of hydroxyl groups in the polymer structure [39].

3.2 Physical and Chemical Characterization

The sample had a homogeneous granular appearance, a yellowish color, and was odorless. The moisture content was determined to be 6.57 ± 0.05%, a value considered low and favorable for the stability of polysaccharides, as it contributes to their preservation [31]. The pH of the aqueous polysaccharide solution was 6.94 ± 0.34, indicating a slightly acidic to nearly neutral character.

3.3 Infrared spectroscopy

The structural characterization of the polysaccharide was performed using Fourier-transform infrared (FTIR) spectroscopy (Figure 1). The spectrum revealed a broad band in the 3000–3600 cm^{-1} region, attributed to O–H stretching, indicating the presence of hydroxyl groups in the sample. This characteristic is typical of hygroscopic biopolymers and reinforces the polysaccharide's high affinity for water, consistent with the behavior observed in the solubility and swelling tests [7].

Another band, located at approximately 2900 cm^{-1}, corresponds to the stretching of C–H bonds, confirming the presence of organic chains in the structure. In the 1600–1650 cm^{-1} region, a band attributed to the bending of adsorbed water molecules (H–O–H) was observed. This absorption is frequently reported in spectra of apple pectin and pectins extracted from citrus peels, thus constituting a recurring band in polysaccharides, including pectins [38]. This is shown in Figure 1:

Figure 1 - FTIR spectrum of the polysaccharide from the pseudofruit residue of *Anacardium occidentale*. FTIR spectrum (transmittance × wavenumber) of the sample studied. Notable bands are observed at 1000–1200 cm^{-1} (C–O vibrations), 1400 cm^{-1} (C–H bending), 1600 cm^{-1} (adsorbed water), 2900 cm^{-1} (C–H stretching), and 3000–3600 cm^{-1} (O–H stretching).

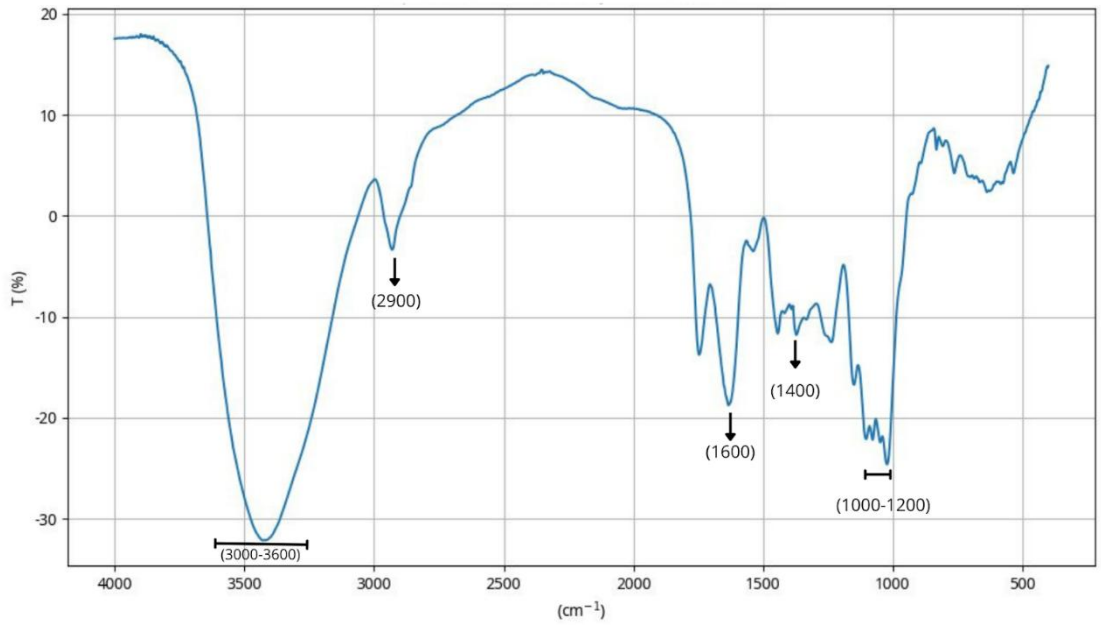

In the 1400–1450 cm^{-1} region, bands attributed to the deformation vibrations of CH_2 or carboxylate ($–COO^-$) groups were identified; these findings are similar to those reported for plant exudate gums, which exhibit a characteristic band at 1424 cm^{-1} [76].

The 1000–1200 cm^{-1} range, in turn, is representative of the vibrations of C–O and C–C bonds and glycosidic bonds, in addition to reflecting specific movements of the pyranose and furanose rings, confirming the polysaccharide nature of the sample [29]. The bands observed below 700 cm^{-1} are associated with vibrations of the molecular backbone and other structural deformations of lower intensity, complementing the chemical characterization [74].

The results obtained are consistent with those described by [64], who reported an O–H stretch in the 3000–3500 cm^{-1} region, as well as a C–H stretch of the $–CH_2–$ groups at 2930 cm^{-1}. Similarly, pectin extracted from *A. occidentale* residue exhibited a C=O stretch at 1742 cm^{-1} [20], while the gum derived from the same plant species exhibited C–O stretching bands at 1070 and 1151 cm^{-1}, characteristic of fundamental bonds in the composition of polysaccharides [27].

3.4 Scanning Electron Microscopy (SEM)

The micrograph reveals the presence of fragments that are predominantly lamellar in shape (in “plates”) and some more irregular agglomerates, as shown in Figure 2-D. The topography of the particles is characterized as rough, with irregular surfaces and fissures (Figure 2-A).

Figure 2 - SEM images showing the morphology of *A. occidentale* polysaccharide particles at different magnifications. A) 20,000x, B) 10,000x, C) 5,000x, D) 1,000x.

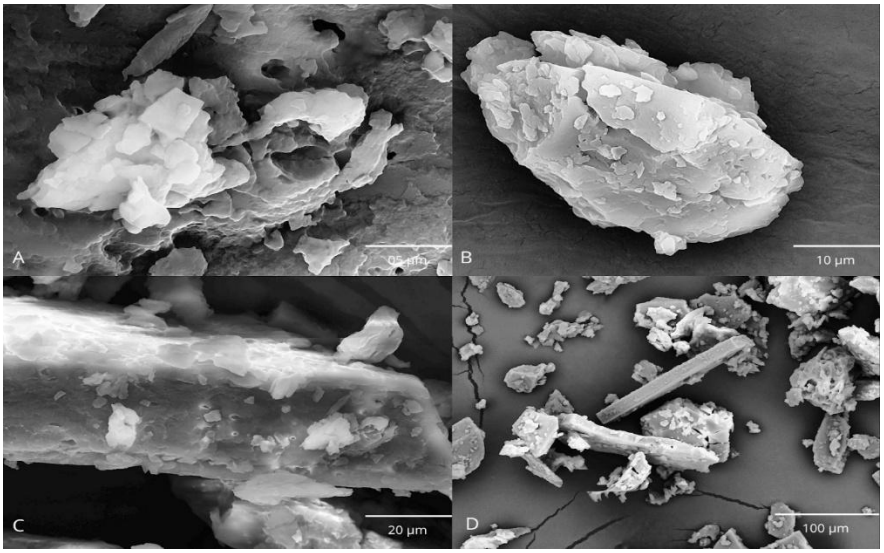

In some areas, overlapping layers are visible, suggesting a possible laminar or stratified structure (Figures 2-B and 2-C). The presence of fractures or thinner edges may be related to the drying or grinding process, which often produces cracks and fragments [64]. When analyzing the polysaccharide extracted from *Anacardium occidentale* residue, the authors reported a compact and slightly wrinkled morphology, without pores or bubbles, indicating that the temperature used in the extraction preserved the surface structures.

In turn [1], the authors described the lignin extracted from *A. occidentale* bagasse as having a heteropolymetric, amorphous, and three-dimensional morphology. This analysis is an important tool for characterizing the morphology of polysaccharides, as it allows for the visualization of structures on a micrometric scale [23].

3.5 X-ray Fluorescence (XRF)

X-ray fluorescence (XRF) analysis shown in Figure 3 revealed that the predominant elements in the polysaccharide sample are potassium (K), calcium (Ca), and phosphorus (P), with lower concentrations of silicon (Si), sulfur (S), and magnesium (Mg). In addition, nickel (Ni), chromium (Cr), and manganese (Mn) were detected as trace elements.

Similar results were observed by [45] in their X-ray microfluorescence analysis using gum from *A. occidentale*, which showed higher concentrations of calcium, potassium, magnesium, and manganese; this similarity is due to their shared plant origin. These elements are often associated with natural mineral constituents of plant biomass or with the residual

Figure 3 - X-ray fluorescence (XRF). A) XRF spectrum of the polysaccharide sample; B) Elemental composition profile, showing the main elements detected.

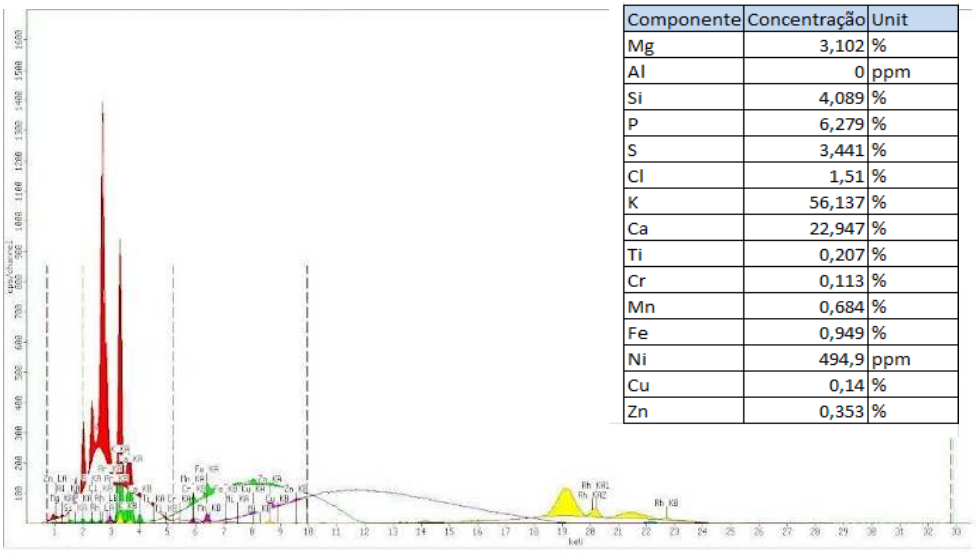

Componente	Concentração	Unit
Mg	3,102	%
Al	0	ppm
Si	4,089	%
P	6,279	%
S	3,441	%
Cl	1,51	%
K	56,137	%
Ca	22,947	%
Ti	0,207	%
Cr	0,113	%
Mn	0,684	%
Fe	0,949	%
Ni	494,9	ppm
Cu	0,14	%
Zn	0,353	%

3.6 Thermogravimetric Analysis

The thermogravimetric profile, as shown in Figure 4, revealed that the first stage of degradation occurred up to approximately 150 °C. A mass loss was observed, attributed to the evaporation of adsorbed moisture and volatile compounds present on the material's surface. Subsequently, in the 200–350 °C range, the initial decomposition of the polysaccharide chains occurred—a process characteristic of the thermal degradation of biopolymers, in which glycosidic bonds break and volatile byproducts are formed.

Figure 4 - Mass loss curve of the *Anacardium occidentale* polysaccharide obtained by TG.

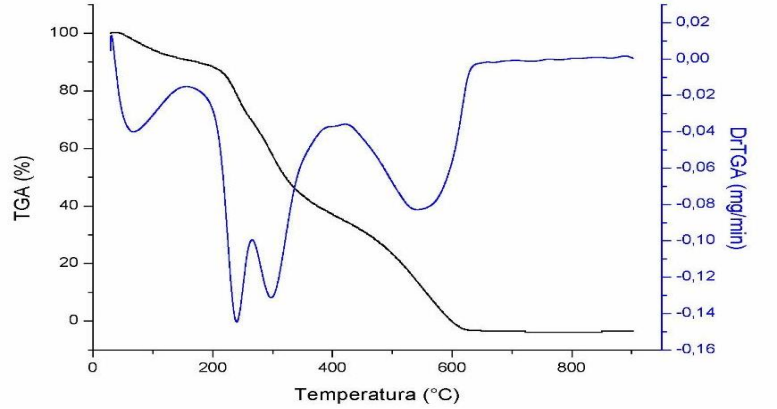

The thermogravimetric profile of the polysaccharide (Figure 4) revealed an initial stage of thermal degradation up to approximately 150 °C, associated with mass loss resulting from the evaporation of adsorbed moisture and surface volatile compounds. In the 200–350 °C range, the initial decomposition of the polysaccharide chains was observed, an event typical of the thermal degradation of biopolymers, characterized by the breaking of glycosidic bonds and the formation of volatile byproducts.

Between 350 and 550 °C, the degradation process continued, likely related to the decomposition of more recalcitrant polymeric fragments and residual carbonaceous structures. Above 600 °C, a significant amount of thermal residue was observed, consistent with the material's high mineral content. This result is consistent with the XRF analysis, which revealed the presence of elements such as calcium (Ca), potassium (K), and phosphorus (P), which are generally associated with the inorganic fraction of biomass and ash content.

Similar profiles were reported by [64], who observed degradation ranges close to those described in this study. [45] also reported analogous behavior for *A. occidentale* gum, with thermal degradation beginning at 195 °C. According to these authors, the 200 °C range is related to the degradation of hemicelluloses, while cellulose decomposition occurs between 300 and 380 °C.

3.7 Antioxidant activity

The polysaccharide from *A. occidentale* had an effective concentration (EC50) of 0.5688 ± 0.01 mg/mL for inhibiting 50% of DPPH• free radicals, compared to the standards ascorbic acid (EC50 = 0.0227 ± 0.00 mg/mL) and Trolox® (EC50 = 0.0149 ± 0.00 mg/mL), demonstrating that the polysaccharide exhibits greater antioxidant capacity than the standards against DPPH•. This polysaccharide was also tested for its total antioxidant activity using the ABTS•+ radical by [64], where the antioxidant activity found was 147 µM of Trolox/g, corresponding to an ABTS• + of 89% at a concentration of 0.05 mg/mL, reinforcing the polysaccharide's scavenging potential even at low concentrations.

3.8 Antibacterial activity

The test results showed that none of the concentrations tested exhibited activity against the standard E. coli strain, with the minimum inhibitory concentration (MIC) for the polysaccharide being greater than 100 µg/mL (0.01%). To date, no similar study has been reported in the literature for this particular polysaccharide. [1] conducted an antimicrobial activity assay using lignin from the fibrous residue of *A. occidentale*, demonstrating dose-dependent activity against these strains, with total inhibition at 3% (w/v) lignin, reaching 100% activity at a concentration of 10% (w/v) lignin for E. coli and 5% for S. aureus.

Other parts of the species *A. occidentale*, such as the extract from the nut shell, exhibit activity against strains of S. aureus (MIC 25 mg/mL) [54], while the gum from the exudate has an MIC of 30 mg/mL against E. coli [11]. This indicates the need for further testing to determine the minimum inhibitory concentration for the extracted polysaccharide.

3.9 In vitro toxicity

In vitro toxicity testing of the polysaccharide was conducted using Artemia salina nauplii, revealing a low toxicity profile at concentrations ranging from 250 to 2000 µg mL^{-1}, with values close to those of the negative control, as shown in Figure 5, where the mortality rate ranged from 0% to 15%.

Figure 5 - Mortality after 24/48 hours of exposure. CP – Positive control ($K_2Cr_2O_7$, 10 µg mL^{-1}), CN – Negative control, artificial seawater only.

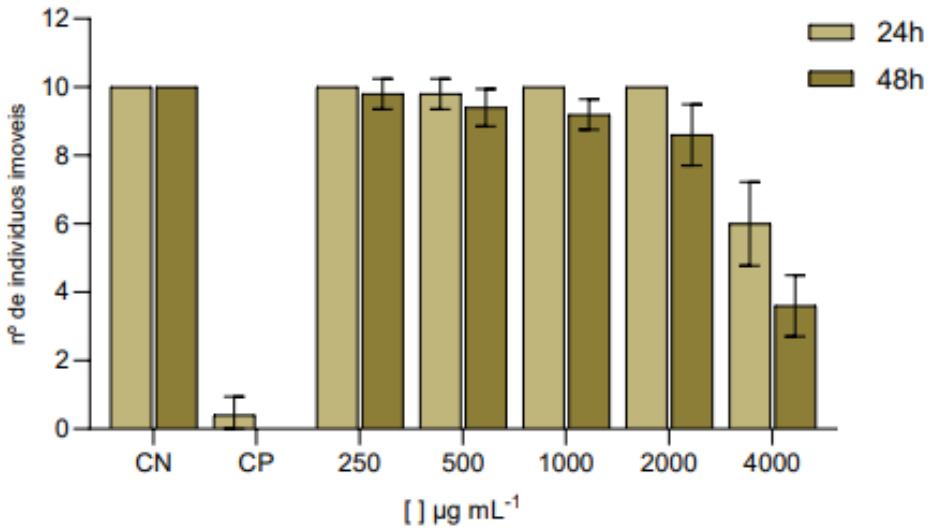

This indicates that, at moderate concentrations, polysaccharides do not exhibit any toxic effects and can be used safely. However, at a concentration of 4000 µg mL^{-1}, a significant reduction in the number of individuals was observed, indicating increased mortality, reaching approximately 40% after 24 hours and exceeding 60% after 48 hours of exposure (Figure 6), with a significant difference compared to lower concentrations.

The test results showed that the median lethal concentration (LC_{50}) after 24 hours of exposure was 11.283 µg/mL (95% confidence interval: 7.834–17.983 µg/mL) and after 48 hours was 4.911 µg/mL (95% CI: 3.624 – 6.895 µg/mL). Thus, the analyzed polysaccharide is considered to have low toxicity, according to the scale proposed by Clarkson, in which substances with an LC_{50} equal to or greater than 1000 µg/mL are considered weakly toxic [26];

Figure 6 - Mortality after 24/48 hours of exposure.

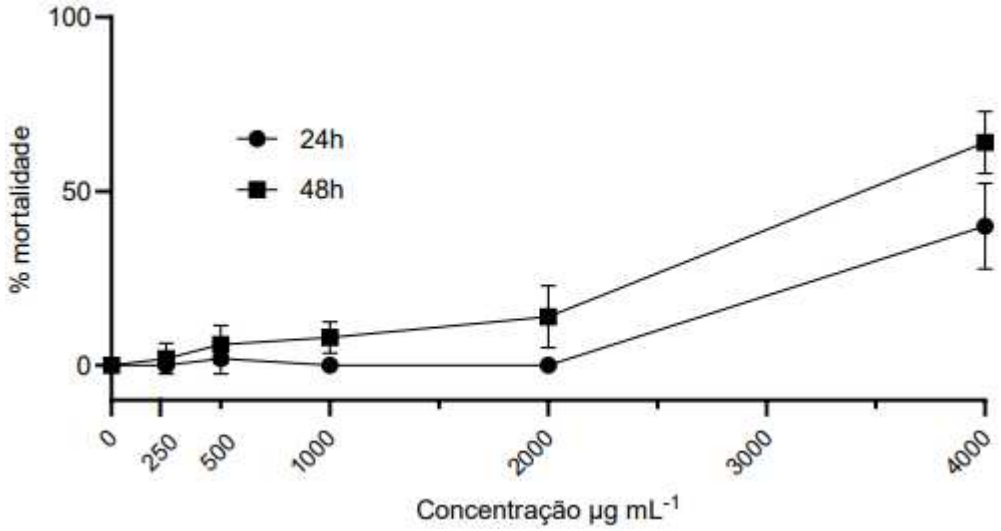

The polysaccharide from *A. occidentale* residue exhibited higher apparent toxicity compared to the sulfated polysaccharide from Ulva, whose LC50 was 15,815.85 ppm after 24 hours of exposure, while mortality rates ranged from 9.33% (625 ppm) to 41.33% (5,000 ppm), demonstrating a dose-dependent pattern [2].

Similarly, the increase in toxicity at higher concentrations of the polysaccharide from *A. occidentale* residue—particularly at the highest concentrations—may be related to physical effects caused by the suspension's high colloidal density, since high concentrations of the polymer in solution can increase its viscosity, hindering oxygen diffusion and causing the nauplii to suffocate [67]. This does not reflect the toxicity of the sample, but rather environmental stress.

3.10 *Scaffold* production

The scaffolds were obtained from the polysaccharide extracted from the fibrous residue of *Anacardium occidentale*, which was used as the main component of the formulation. Production was carried out using the freeze-drying technique, widely employed to generate porous matrices from hydrogels. In this process, free and bound water is solidified, and ice crystals act as porogen agents; during expansion, the polymer expels the ice, resulting in a continuous network of interconnected pores [24].

The choice of this polymer is based on its sustainable nature and its potential for biomedical applications. Xanthan gum was incorporated as a gelling agent, enabling the formation of the hydrogel, and three different concentrations were evaluated to investigate their influence on the structural properties of the final formulation.

The resulting scaffolds exhibited a homogeneous morphology, a yellowish color typical of *A. occidentale* polymer, were odorless, and had a cylindrical shape with an average diameter of 0.83 ± 0.06 mm (Figure 7). From a macroscopic perspective, the SCF-P3 formulation, with the highest concentration of xanthan gum, exhibited a more compact and dense structure, whereas the SCF-P1 formulation had a lighter appearance and greater porosity (Figure 7).

Figure 7 - Scaffold developed from polysaccharide derived from the fibrous waste of *A. occidentale*, formulation SCF-P1. A) Side view; B) Top view.

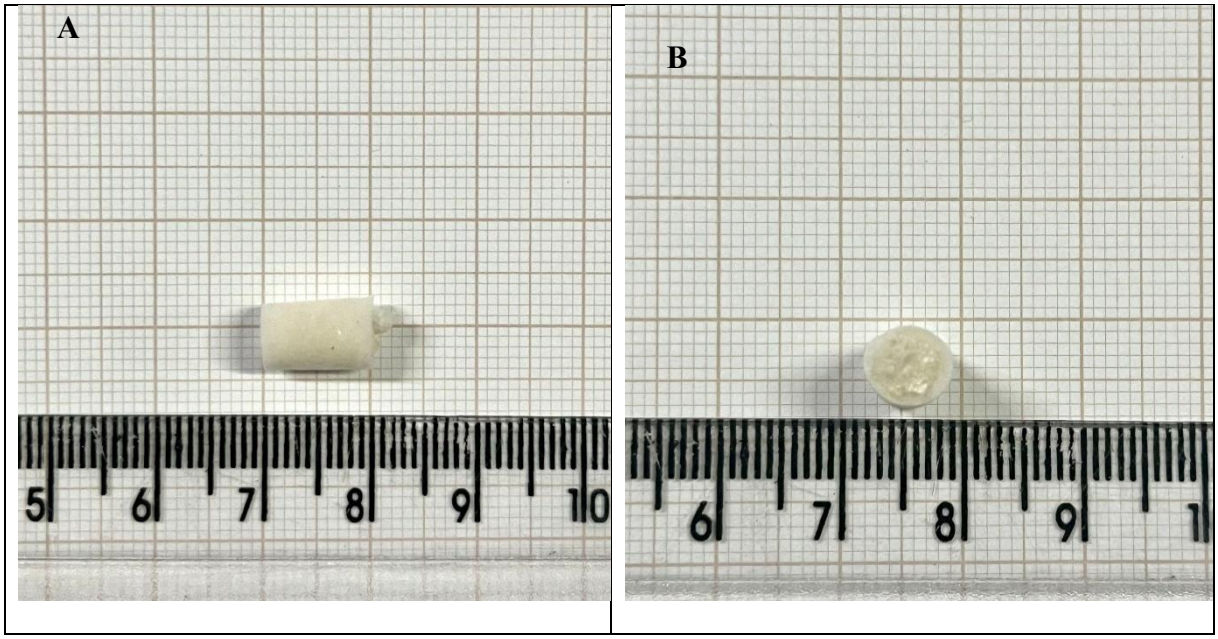

3.11 Computed Microtomography

Microtomography was used to evaluate the three-dimensional architecture of the scaffold and reveal the internal structure of the developed scaffolds. The main morphometric parameters are shown in Figure 8.

Figure 8 - Images obtained by computed microtomography. A and B) 0.5% xanthan gum scaffold. C and D) 1% xanthan gum scaffold. E and F) 2% xanthan gum scaffold.

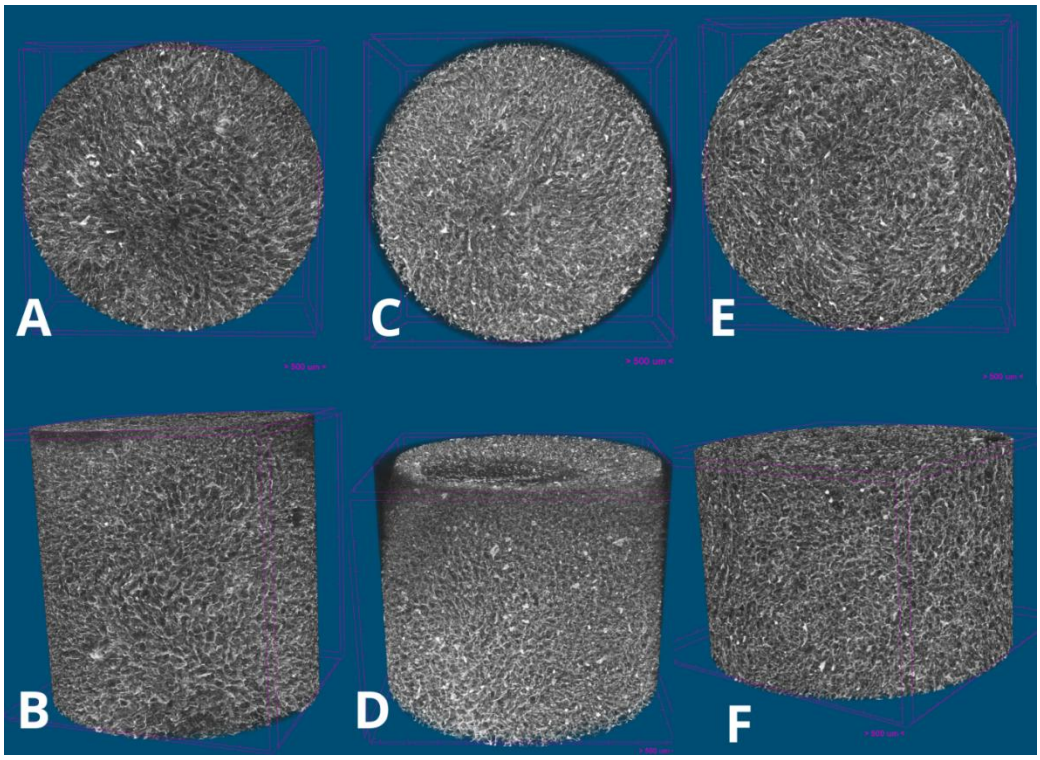

The SCF-P1 and SCF-P2 scaffolds exhibited higher porosity, with mean values of 96.06 ± 5.28% and 97.59 ± 3.34%, respectively, as evidenced by images A–D, which show a porous and relatively low-density structure with a large number of interconnected pores. Meanwhile, SCF-P3 exhibited the lowest porosity (88.31 ± 1.17%) and a more compact morphology, with smaller, more compact, and more homogeneous pores; these morphological characteristics corroborate the visual observations of the scaffolds. High porosity is one of the ideal characteristics of a scaffold, as it facilitates cellular integration of the biomaterial with the target tissue, in addition to enabling nutrient diffusion and gas exchange [10].

Scaffolds with porosity greater than 90% can be used for the delivery of cells and drugs, as they facilitate the entry of fluids, accelerating the dissolution of the active ingredient incorporated into the polymer matrix—ideal for immediate release [6]. Less porous scaffolds, such as SPC-P3, have a higher solid content and lower porosity; they favor sustained drug release by limiting the rapid entry of fluids. Thus, porosity influences the release rate of the incorporated drug [80].

The formulations exhibited different porosity percentages due to the concentration of xanthan gum; the more viscous hydrogel produced fewer pores during freeze-drying. A similar behavior was observed by Samourides et al. [70], where the scaffolds produced exhibited lower porosity as the polymer concentration increased. The minimum porosity required for scaffolds is 80%; thus, all three formulations meet this requirement [37].

3.12 Scanning electron microscopy

Morphological analysis by scanning electron microscopy revealed that the SCF-P1 scaffold has a three-dimensional porous structure with an irregular distribution (Figure 9-A) and interconnected pores.

Figure 9 - Particle morphology of the xanthan gum *scaffold.* A) 0.5% xanthan gum scaffold at scales of 50 µm, 20 µm, and 100 µm. D) 1% xanthan gum scaffold: 50 µm, 20 µm, 100 µm. E and F) 2% xanthan gum scaffold: 50 µm, 20 µm, 100 µm.

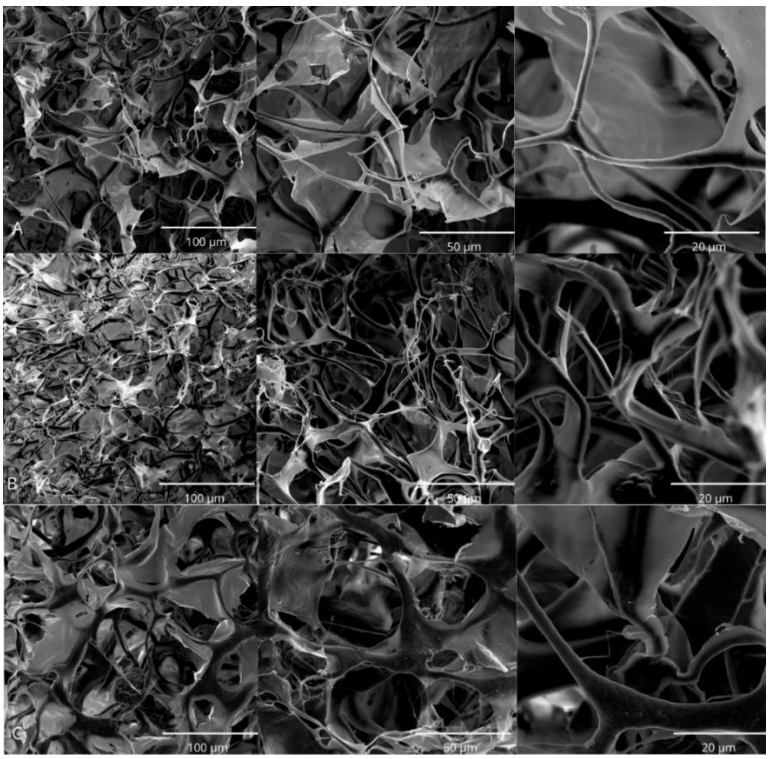

This characteristic is essential for biomedical applications, as it promotes the diffusion of biological fluids and active substances, as well as gas exchange [52]. The pores vary in size and have thin walls, forming lamellae and network structures, which may be related to the interaction between the polysaccharide from *A. occidentale* and xanthan gum, since the presence of natural gums increases the hydrogel's viscosity during scaffold production, resulting in a more stable matrix after lyophilization [18]; these characteristics influence the scaffold's application, resulting in a sustained-release profile but with heterogeneous diffusion [14].

The SCF-P2 formulation exhibited similar porosity; however, it featured a more homogeneous and interconnected three-dimensional network with thin, rough walls. This morphology favors fluid permeation and cell migration, indicating a profile suitable for applications requiring high permeability and diffusion—ideal for the release of active ingredients with a more pronounced initial release, followed by a more sustained release [5]. In contrast, the SCF-P3 formulation has an irregular and robust structure, with connected pores but thicker lamellar networks; some regions exhibited overlapping layers, resulting in greater roughness and mechanical strength, which is favorable for slower, continuous sustained release [14,16].

3.12 *Ex vivo mucoadhesion*

In the present study, the SCF-P1 formulation exhibited the highest adhesive strength (0.0925 ± 0.0159 $N \cdot cm^{-2}$) (Table 1), possibly due to its polymer composition. This behavior can be explained by the fact that mucoadhesive forces depend on chemical interactions between the polymer and the mucosa, particularly hydrogen bonds and weak van der Waals interactions [60].

The high porosity of the scaffold may also have contributed to the higher adhesiveness, promoting close contact between the biomaterial and the mucosa by increasing permeability [61]. On the other hand, the SCF-P2 (0.0447 ± 0.0030 $N \cdot cm^{-2}$) and SCF-P3 (0.0439 ± 0.0180 $N \cdot cm^{-2}$) formulations exhibited values similar to those of the control formulation SCF -C1 (0.0479 ± 0.0133 $N \cdot cm^{-2}$), suggesting that the increased concentration of xanthan gum resulted in lower adhesiveness. This effect can be attributed to the more compact morphology of the scaffolds, which limits interaction with the mucosal surface [52].

The formulations containing fluconazole exhibited the lowest mean mucoadhesion values, with the lowest value observed for the SCF-F3 scaffold (0.0257 ± 0.0095 $N \cdot cm^{-2}$). The presence of the drug in the formulation may have influenced mucoadhesivity by reducing the availability of functional groups that interact with the mucosa [34]. Different results were reported by Pahwa and Ahuja [59], who developed rice and wheat nanocellulose scaffolds combined with gellan gum, achieving mucoadhesion values of 830 ± 150 mN and 870 ± 190 mN, respectively. Furthermore, the scaffolds incorporated with fluconazole and cross-linked with trisodium trimetaphosphate exhibited significantly higher values, reaching 2160 ± 200 mN for the rice nanocellulose formulation and 1940 ± 220 mN for the wheat nanocellulose formulation.

Although the units of measurement for mucoadhesion vary across studies, it is observed that the use of crosslinking agents substantially increases interaction with the mucosa. These findings suggest that, to optimize the mucoadhesive properties of the polysaccharide extracted from *A. occidentale* residue, strategies such as

increasing the polymer concentration, chemical modifications (e.g., the introduction of thiol groups), or replacing xanthan gum with polymers that have greater mucoadhesive affinity may be promising alternatives [13].

4. Conclusion

In light of this, the fibrous residue from the pseudofruit of *Anacardium occidentale* is a promising source for polysaccharide extraction using the hot-water method followed by ethanol recovery, yielding a 2.54 ± 1.54% yield. The obtained polysaccharide exhibited functional groups characteristic of polysaccharides, with potassium, calcium, and phosphorus as the predominant elements in its composition. It has a plate-like morphology, with a rough topography and an irregular surface, as well as good thermal stability at low and medium temperatures, the ability to scavenge free radicals, and low toxicity.

From the extracted polysaccharide, it was possible to obtain scaffolds with high porosity, featuring interconnected pores that facilitate drug release, and low mucoadhesiveness—a property that can be improved through modification of the polysaccharide. These results highlight the potential for using these residues to produce polysaccharides, adding value to the cashew production chain and yielding a material with potential applications in pharmaceutical formulations.

5. Funding

The authors received no financial support for the research, authorship, and/or publication of this article.

References

[1] T.L. Albuquerque, et al., Hydrogels based on lignin extracted from cashew apple bagasse and its application in antimicrobial wound dressings, Int. J. Biol. Macromol. 262 (2024) 130169.

[2] A. Alves, R.A. Sousa, R.L. Reis, In vitro cytotoxicity assessment of ulvan, a polysaccharide extracted from green algae, Phytother. Res. 27 (8) (2013) 1143–1148.

[3] A.J. Antonisamy, et al., Sustainable approaches on industrial food wastes to value-added products – A review on extraction methods, characterizations, and its biomedical applications, Environ. Res. 217 (2023) 114758.

[4] C.M. Araújo, et al., Cashew-gum-based silver nanoparticles and palygorskite as green nanocomposites for antibacterial applications, Mater. Sci. Eng. C 115 (2020) 110927.

[5] S. Asikainen, et al., Hydrolysis and drug release from poly(ethylene glycol)-modified lactone polymers with open porosity, Eur. Polym. J. 113 (2019) 165–175.

[6] A. Autissier, et al., Fabrication of porous polysaccharide-based scaffolds using a combined freeze-drying/cross-linking process, Acta Biomater. 6 (9) (2010) 3640–3648.

[7] A. Basu, et al., Polysaccharide-Based Conjugates for Biomedical Applications, Bioconjug. Chem. 26 (8) (2015) 1396–1412.

[8] W. Brand-Williams, M.E. Cuvelier, C. Berset, Use of a free radical method to evaluate antioxidant activity, LWT Food Sci. Technol. 28 (1) (1995) 25–30.

[9] Brasil. Agência Nacional de Vigilância Sanitária, Farmacopeia Brasileira, 7th ed., Anvisa, Brasília, 2019.

[10] I.R. Calori, et al., Polymer scaffolds as drug delivery systems, Eur. Polym. J. 129 (2020) 109621.

[11] D.A. Campos, et al., Study of antimicrobial activity and atomic force microscopy imaging of the action mechanism of cashew tree gum, Carbohydr. Polym. 90 (1) (2012) 270–274.

[12] C.M. Caramella, et al., Mucoadhesive and thermogelling systems for vaginal drug delivery, Adv. Drug Deliv. Rev. 92 (2015) 39–52.

[13] I.S. Cho, et al., Synthesis and characterization of thiolated hexanoyl glycol chitosan as a mucoadhesive thermogelling polymer, Biomater. Res. 22 (1) (2018).
[14] H.J.B. Chua, et al., Visible light-based three-dimensional printing of drug-loaded scaffolds: a comparative study of initiating systems and drug release profiles, ACS Appl. Polym. Mater. 6 (17) (2024) 10853–10864.

[15] H.J. Chung, T.G. Park, Surface engineered and drug releasing pre-fabricated scaffolds for tissue engineering, Adv. Drug Deliv. Rev. 59 (4–5) (2007) 249–262.

[16] J.A. da Costa, et al., Enhanced enzymatic hydrolysis and ethanol production from cashew apple bagasse pretreated with alkaline hydrogen peroxide, Bioresour. Technol. 179 (2015) 249–259.

[17] H.P. Dang, et al., 3D printed dual macro-, microscale porous network as a tissue engineering scaffold with drug delivering function, Biofabrication 11 (3) (2019) 035014.

[18] G.G. da Silva, et al., Cashew apple byproduct: Gastroprotective effects of standardized extract, J. Ethnopharmacol. 269 (2021) 113744.

[19] K.C. da Silva, et al., Mapeamento tecnológico da espécie Anacardium occidentale: análise prospectiva no Brasil e no mundo, Res. Soc. Dev. 11 (4) (2022) e47511427669.

[20] I. del Agua, et al., Conducting polymer scaffolds based on poly(3,4-ethylenedioxythiophene) and xanthan gum for live-cell monitoring, ACS Omega 3 (7) (2018) 7424–7431.

[21] C.S.V. de Menezes, et al., Extraction of cell wall pectins and hemicellulose from agroindustrial wastes: A sustainable alternative source, Carbohydr. Polym. 347 (2024) 122769.

[22] A.L. de Vasconcelos, et al., Microscopic and histochemical characterization applied to quality control of Anacardium occidentale, S. Afr. J. Bot. 171 (2024) 748–756.

[23] C.O. Dimkpa, P.S. Bindraban, Fortification of micronutrients for efficient agronomic production: a review, Agron. Sustain. Dev. 36 (1) (2016) 7.

[24] M. Filippi, et al., Natural Polymeric Scaffolds in Bone Regeneration, Front. Bioeng. Biotechnol. 8 (2020).

[25] E.R. Fischer, et al., Scanning Electron Microscopy, Curr. Protoc. 4 (5) (2024).

[26] J. Grenier, et al., Mechanisms of pore formation in hydrogel scaffolds textured by freeze-drying, Acta Biomater. 94 (2019) 195–203.

[27] C. Gutiérrez-Paz, et al., The Cashew Pseudofruit (Anacardium occidentale): Composition, Processing Effects on Bioactive Compounds and Potential Benefits for Human Health, Foods 13 (15) (2024) 2357.

[28] M.Q. Guo, et al., Polysaccharides: structure and solubility, Solubility Polysaccharides 2 (2017) 8–21.

[29] M.R. Hamidi, B. Jovanova, T.K. Panovska, Toxicological evaluation of the plant products using Brine Shrimp (Artemia salina L.) model, Maced. Pharm. Bull. 60 (1) (2014) 9–18.

[30] M.S. Hasnain, et al., Extraction and characterization of cashew tree (Anacardium occidentale) gum; use in aceclofenac dental pastes, Int. J. Biol. Macromol. 116 (2018) 1074–1081.

[31] S. Jain, et al., Potential of natural polymeric materials in pharmaceutics, Pharmacol. Res. Nat. Prod. 2 (2024) 100014.

[32] Z. Jawadi, et al., Bio-inspired muco-adhesive polymers for drug delivery applications, Polymers 14 (24) (2022) 5459.

[33] K. Jeyavishnu, et al., Increased Revenue with High Value-Added Products from Cashew Apple (Anacardium occidentale L.)—Addressing Global Challenges, Food Bioprocess Technol. 14 (6) (2021) 985–1012.

[34] M. José, et al., Lyophilized tablets for focal delivery of fluconazole and itraconazole through vaginal mucosa: rational design and in vitro evaluation, Eur. J. Pharm. Sci. 122 (2018) 144–151.

[35] M. Kacurakova, et al., FT-IR study of plant cell wall model compounds: pectic polysaccharides and hemicelluloses, Carbohydr. Polym. 43 (2) (2000) 195–203.

[36] S. Khademolqorani, et al., The determinant role of fabrication technique in final characteristics of scaffolds for tissue engineering applications: A focus on silk fibroin-based scaffolds, Mater. Sci. Eng. C 122 (2021) 111867.

[37] L. Kong, et al., Physicochemical characterization of the polysaccharide from Bletilla striata: Effect of drying method, Carbohydr. Polym. 125 (2015) 1–8.

[38] O.M. Kolawole, P.K. Okeke, Formulation and Evaluation of boronated 4-arm polyethylene glycol/polyvinyl pyrrolidone/methylcellulose-based fluconazole films for the Potential Treatment of Vaginal Candidiasis, J. Drug Deliv. Sci. Technol. 107 (2025) 106838.

[39] A. Kuila, et al., Process optimization for aqueous extraction of reducing sugar from cashew apple bagasse: A potential, low cost substrate, LWT Food Sci. Technol. 44 (1) (2011) 62–66.

[40] D. Kunjumon, A.M. Shenoy, Anacardium occidentale (Linn): A Brief Review, Int. J. Pharm. Sci. Rev. Res. (2022) 6–9.

[41] J.H. Li, et al., Efficient isolation of immunostimulatory polysaccharides from Lentinula edodes by autoclaving-ultrasonication extraction and fractional precipitation, Int. J. Biol. Macromol. 237 (2023) 124216.

[42] S. Liu, et al., Preparation and sustained-release properties of poly(lactic acid)/graphene oxide porous biomimetic composite scaffolds loaded with salvianolic acid B, RSC Adv. 12 (45) (2022) 28867–28877.

[43] X. Liu, et al., Revisiting the contribution of ATR-FTIR spectroscopy to characterize plant cell wall polysaccharides, Carbohydr. Polym. 262 (2021) 117935.

[44] L. Llanes, et al., Biosourced Polysaccharide-Based Superabsorbents, Polysaccharides 1 (1) (2020) 51–79.

[45] J.E. Marques Júnior, M.V.P. Rocha, Development of a purification process via crystallization of xylitol produced for bioprocess using a hemicellulosic hydrolysate from the cashew apple bagasse as feedstock, Bioprocess Biosyst. Eng. 44 (4) (2021) 713–725.

[46] J.C. McLaughlin, Crown gall tumors on potato discs and brine shrimp lethality: Two brine shrimp bioassays for higher plant screening, Methods Biochem. Assays Bioact. 6 (1991) 1–32.

[47] B.N. Meyer, N.R. Ferrigni, J.E. Putnam, L.B. Jacobsen, D.E. Nichols, J.L. McLaughlin, Brine shrimp: a convenient general bioassay for active plant constituents, Planta Med. 45 (5) (1982) 31–34.

[48] J.J. Mathavan, M.H. Bin Hassan, Thermal–chemical–mechanical characterization of Anacardium occidentale tree gum, Int. J. Biol. Macromol. 271 (2024) 132396.

[49] Y. Meng, et al., Density-oriented deep eutectic solvent-based system for the selective separation of polysaccharides from Astragalus membranaceus var. Mongholicus under ultrasound-assisted conditions, Ultrason. Sonochem. 98 (2023) 106522.

[50] C.C. Mohan, et al., Extraction and characterization of polysaccharides from tamarind seeds, rice mill residue, okra waste and sugarcane bagasse for its bio-thermoplastic properties, Int. J. Biol. Macromol. 186 (2018) 394–401.

[51] B. Mohankumar, et al., Vaginosis: Advances in new therapeutic development and microbiome restoration, Microb. Pathog. 168 (2022) 105606.

[52] F. Mukasheva, et al., Design and characterization of 3D printed pore gradient hydrogel scaffold for bone tissue engineering, Bioprinting 39 (2024) e00341.

[53] E.M. Nsengiyumva, P. Alexandridis, Xanthan gum in aqueous solutions: Fundamentals and applications, Int. J. Biol. Macromol. 216 (2022) 583–604.

[54] T.P. Nguyễn, et al., Antimicrobial activity of cashew nut testa extract (Anacardium occidentale L.), Tap Chi Nong Nghiep va Phat Trien 23 (Special Issue 2) (2024) 155–165.

[55] N.N. Oliveira, et al., Cashew nut and cashew apple: a scientific and technological monitoring worldwide review, J. Food Sci. Technol. 57 (1) (2020) 12–21.

[56] D.H. Owen, D.L. Katz, A vaginal fluid simulant, Contraception 59 (2) (1999) 91–95.

[57] R. Pahwa, M. Ahuja, Nanocellulose-gellan cross-linked scaffolds for vaginal delivery of fluconazole, Int. J. Biol. Macromol. 229 (2022) 668–683.

[58] G.L. Pérez-González, et al., Mucoadhesive electrospun nanofibers for drug delivery systems: applications of polymers and the parameters' roles, Int. J. Nanomedicine 14 (2019) 5271–5285.

[59] R.A. Perez, G. Mestres, Role of pore size and morphology in musculo-skeletal tissue regeneration, Mater. Sci. Eng. C 61 (2016) 922–939.

[60] M. Prabaharan, R. Jayakumar, Chitosan-graft-β-cyclodextrin scaffolds with controlled drug release capability for tissue engineering applications, Int. J. Biol. Macromol. 44 (4) (2009) 320–325.

[61] R. Rajesh, Y.D. Ravichandran, Development of a new carbon nanotube–alginate–hydroxyapatite tricomponent composite scaffold for application in bone tissue engineering, Int. J. Nanomedicine 10 (Suppl. 2) (2015) 7–15.

[62] M.S.B. Reddy, et al., A Comparative Review of Natural and Synthetic Biopolymer Composite Scaffolds, Polymers 13 (7) (2021) 1105.

[63] C. Rhamon, et al., Synthesis and characterization of scaffolds produced under mild conditions based on oxidized cashew gums and carboxyethyl chitosan, Int. J. Biol. Macromol. 176 (2021) 26–36.

[64] B.S. Sabino, et al., Polysaccharides from acerola, cashew apple, pineapple, mango and passion fruit co-products: Structure, cytotoxicity and gastroprotective effects, Bioact. Carbohydr. Diet. Fibre 24 (2020) 100228.

[65] D.F. Sahm, Antibacterial susceptibility tests: dilution methods, in: Manual of Clinical Microbiology, 1995.

[66] A. Samourides, et al., The effect of porous structure on the cell proliferation, tissue ingrowth and angiogenic properties of poly(glycerol sebacate urethane) scaffolds, Mater. Sci. Eng. C 108 (2020) 110384.

[67] G. Salay, et al., Acute toxicity assays with the Artemia salina model: Assessment of variables, Altern. Lab. Anim. 52 (3) (2024) 142–148.

[68] B. Salehi, et al., Anacardium Plants: Chemical, Nutritional Composition and Biotechnological Applications, Biomolecules 9 (9) (2019) 465.

[69] R.M. Schweiggert, et al., Carotenoids, carotenoid esters, and anthocyanins of yellow-, orange-, and red-peeled cashew apples (Anacardium occidentale L.), Food Chem. 200 (2016) 274–282.

[70] Á. Serrano-Aroca, et al., Scaffolds in the microbial resistant era: Fabrication, materials, properties and tissue engineering applications, Mater. Today Bio 16 (2022) 100412.

[71] L. Shang, S. Wang, Y. Mao, Recent advances in plant-derived polysaccharide scaffolds in tissue engineering: A review, Int. J. Biol. Macromol. 277 (2024) 133830.

[72] B.A. Sheikh, B.A. Bhat, M.A. Mir, Antimicrobial resistance: new insights and therapeutic implications, Appl. Microbiol. Biotechnol. 106 (19–20) (2022) 6427–6440.

[73] A.C.Q. Silva, et al., Natural Polymers-Based Materials: A Contribution to a Greener Future, Molecules 27 (1) (2021) 94.

[74] J.G.V. Silva, et al., Superabsorbent polyacrylamide nanocomposite hydrogels with cashew tree gum: Investigation of the effect of laponite on swelling capacity and rheological properties, Int. J. Biol. Macromol. 302 (2025) 140487.

[75] M. Szymańska-Chargot, et al., A determination of the composition and structure of the polysaccharides fractions isolated from apple cell wall based on FT-IR and FT-Raman spectra supported by PCA analysis, Food Hydrocoll. 150 (2024) 109688.

[76] S.-H. Teng, et al., Functionally gradient chitosan/hydroxyapatite composite scaffolds for controlled drug release, J. Biomed. Mater. Res. Part B Appl. Biomater. 90B (1) (2008) 275–282.

[77] N. Thombare, et al., Comparative FTIR characterization of various natural gums: a criterion for their identification, J. Polym. Environ. 31 (8) (2023) 3372–3380.

[78] S. Tiwari, R. Patil, P. Bahadur, Polysaccharide Based Scaffolds for Soft Tissue Engineering Applications, Polymers 11 (1) (2019) 1.

[79] L.M. Vieira, M.S.B. Sousa, J. Mancini-Filho, A. Lima, Fenólicos totais e capacidade antioxidante in vitro de polpas de frutos tropicais, Rev. Bras. Frutic. 33 (3) (2011) 888–897.

[80] L.E. Visscher, et al., 3D printed Polycaprolactone scaffolds with dual macro-microporosity for applications in local delivery of antibiotics, Mater. Sci. Eng. C 87 (2018) 78–89.

[81] C. Wang, et al., Extraction and characterization of pectic polysaccharides from Choerospondias axillaris peels: Comparison of hot water and ultrasound-assisted extraction methods, Food Chem. 401 (2023) 134156.

[82] M. Zié, et al., Valorization of cashew apple bagasse in food application: Focus on the use and extraction of nutritional or bioactive compounds, Food Humanit. 1 (2023) 848–863.

[83] Q. Zhang, et al., Electrospun polymeric micro/nanofibrous scaffolds for long-term drug release and their biomedical applications, Drug Discov. Today 22 (9) (2017) 1351–1366.